

## Thermodynamic Simulation of Gas Carburizing of Steels

S. M. H. Modarresi<sup>1\*</sup>, M. Kashefi<sup>2</sup> and J. Vahdati Khaki<sup>3</sup>

Department of Metallurgy and Materials Science Engineering, Ferdowsi University of Mashhad, Mashhad

### Abstract

Simulation of metallurgical processes has been the subject of intense research due to the reduced number of experiments required for controlling the process as well as time and energy savings it allows. In gas carburizing of steel parts, the amount of carbon at the surface of carburized parts is the most important specification of the process in terms of achieving the desired metallurgical properties.

In the present research, the gaseous reactions in an endothermic gas generator have been simulated using MATLAB software where the equilibrium surface carbon percentage was obtained by solving the equilibrium constant equations. The effects such variables as air-to-fuel ratio in the endothermic gas generator, carburizing temperature, pressure inside the furnace, relative humidity, and ambient temperature have been investigated. Besides, working conditions of the furnace have been investigated to obtain the desired carbon potential. Finally, the results of the simulation have been compared with experimental results obtained from a gas carburizing furnace.

**Keywords:** Simulation; Gas carburizing; Carbon percentage; Air-to-fuel ratio; Relative humidity.

### 1- Introduction

Gas carburizing has long been used to improve surface hardness and wear resistance of steel parts. This process is being extensively used for mass production in different industries, especially in automotive parts. Among the parameters affecting the carbon content at the surface of steel, one can name process temperature, furnace pressure, consumed air-to-fuel ratio in the endothermic gas generator, relative humidity, and ambient temperature<sup>1,2</sup>.

A lot of research has been conducted to enhance our understanding of the field by simulating the carburizing process aimed at decreasing production time and increasing process accuracy<sup>3-8</sup>. However, not much of the sort has been done on gas carburizing using the methane gas. F.F.P. De Medeiros is one of the few researchers who have used the methane gas in a gas carburizing process to study the effects of different parameters on the process<sup>9</sup>. Using the thermodynamic simulation of the reactions, he concluded that it is possible to investigate the effects of different variables, such as changes in the furnace as well as environmental factors, on the surface carbon content of steel parts, thereby, optimizing the surface carbon percentage by changing the parameters at minimum time and cost.

\*Corresponding author:

Tel: +98-511-5020464 Fax: +98-511-8763305

E-mail: Mo.Modarresi2003@yahoo.com

Address: Dept. of Metallurgy and Materials Science Engineering, Ferdowsi University of Mashhad, Mashhad

1. M.Sc.

2. Assistant Professor

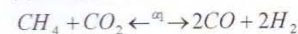
3. Professor

### 2- Experimental Method

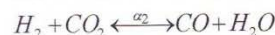
In this study, methane is used as the carburizing gas. It is burned according to reaction (1) in a gas generator and the combustion products enter the furnace chamber<sup>10</sup>.



Combustion products include a mixture of N<sub>2</sub>, CH<sub>4</sub>, H<sub>2</sub>O, H<sub>2</sub>, CO<sub>2</sub>, and CO gases, which are in the equilibrium state according to independent reactions (2) and (3).



$$\Delta G^\circ = 261740 - 285.16T \quad j \quad (2)$$



$$\Delta G^\circ = 34900 - 30.96T \quad j \quad (3)$$

Bearing in mind that the total number of moles in the system equals  $11+x+2\alpha_1$  and using Eqs. 1-3, one can calculate the partial pressure of the gases as follows:

$$P_{CO} = \frac{2\alpha_1 + \alpha_2}{11 + x + 2\alpha_1} P_t$$

$$P_{H_2} = \frac{2\alpha_1 - \alpha_2}{11 + x + 2\alpha_1} P_t$$

$$P_{CO_2} = \frac{1 - \alpha_1 - \alpha_2}{11 + x + 2\alpha_1} P_t$$

$$P_{H_2O} = \frac{2 + \alpha_2}{11 + x + 2\alpha_1} P_t$$

$$P_{CH_4} = \frac{x - \alpha_1}{11 + x + 2\alpha_1} P_t$$

$$P_{N_2} = \frac{8}{11+x+2\alpha_1} \cdot P_t$$

$\alpha_1$  = progress variable of reaction 2  
 $\alpha_2$  = progress variable of reaction 3  
 $P_t$  = total pressure of the furnace

Using the relation  $\Delta G^0 = -RT \ln k$ , Eqs. (4) and (5) are obtained for reactions (2) and (3).

$$\frac{(2\alpha_1 + \alpha_2)^2 (2\alpha_1 - \alpha_2)^2 \cdot P_t^2}{(x - \alpha_1)(1 - \alpha_1 - \alpha_2)(11 + x + 2\alpha_1)^2} = \exp\left(34.3 - \frac{31481838}{T}\right) \quad (4)$$

$$\frac{(2\alpha_1 + \alpha_2) \cdot (2 + \alpha_2)}{(2\alpha_1 - \alpha_2) \cdot (1 - \alpha_1 - \alpha_2)} = \exp\left(3.724 - \frac{4197.739}{T}\right) \quad (5)$$

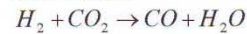
The relationship between the progress of reactions (2) and (3) and the variables total pressure, temperature, and air-to-fuel ratio are given by these equations. As can be seen, the ambient relative humidity is needed to continue with the calculations. The relative humidity is defined as the ratio of steam partial pressure to steam saturation pressure. Eq. 6 expresses the relationship between the saturation pressure of steam and ambient temperature <sup>2)</sup>.

$$P_{H_2O}^{saturation} = \exp\left(\frac{-5417.98}{T_{air}} + 14.736\right) \quad (6)$$

$$\% \text{ humidity} = P_{H_2O}^* / P_{H_2O}^{saturation} \rightarrow$$

$$P_{H_2O}^* = P_{H_2O}^{saturation} \times \text{humidity \%} \quad (7)$$

Now, the partial pressure of steam in the air is added to  $P_{H_2O}$  in the furnace related to reaction (3), as shown below.



$$K = \exp\left(3.724 - \frac{4197.739}{T}\right) = \frac{P_{H_2O} \cdot P_{CO}}{P_{CO_2} \cdot P_{H_2}} = \frac{\left(\frac{2 + \alpha_2 + P_{H_2O}^*}{n_i}\right) \cdot \left(\frac{2\alpha_1 + \alpha_2}{n_i}\right) P_t^2}{\frac{2\alpha_1 - \alpha_2}{n_i} \cdot \frac{1 - \alpha_1 - \alpha_2}{n_i} P_t^2}$$

$$\left\{ \begin{aligned} n_i &= 11 + x + 2\alpha_1 \\ \Rightarrow \exp\left(3.724 - \frac{4197.739}{T}\right) &= \frac{[2 + \alpha_2 + (P_{H_2O}^*/n_i)] \cdot (2\alpha_1 + \alpha_2)}{(2\alpha_1 - \alpha_2) \cdot (1 - \alpha_1 - \alpha_2)} \quad (8) \end{aligned} \right.$$

As a result, the program entries for the calculations will be  $T_{Furnace}$ ,  $P_t$ , air/fuel ratio,  $T_{air}$  and percentage of relative humidity. According to reaction (1), the program obtains  $x$  by using air/fuel ratio shown in Eq. (9).

$$\text{air / fuel ratio} = \frac{2 + 8}{1 + x} \Rightarrow x \text{ is obtained} \quad (9)$$

To obtain the values of  $\alpha_1$  and  $\alpha_2$ , Eqs. (4) and (8) should be solved simultaneously. By substituting the calculated values of  $\alpha_1$  and  $\alpha_2$  in the equations for partial pressures of gases, the equilibrium values for  $P_{CO}$ ,  $P_{CO_2}$ ,  $P_{H_2}$ ,  $P_{H_2O}$ , and  $P_{CH_4}$  will obtain. The carbon activity on the surface of the steel part will be given from Eq. (10) using equilibrium values of  $P_{CO}$ ,  $P_{CO_2}$  in the furnace according to Boudouard reaction.

$$a_c = \frac{P_{CO}^2}{P_{CO_2}} \cdot \exp\left(-20.984 + \frac{20531.63}{T}\right) \quad (10)$$

Finally, using Eq. (11), one can relate carbon activity to its weight percent at the surface of the steel <sup>1)</sup>.

$$\ln a_c = \ln \left[ \frac{4.65w}{100-w} \right] + \frac{9167 \times \left[ \frac{4.65w}{100-w} \right] + 5093}{T} - 1.867 \quad (11)$$

In addition, from Eqs. (12) and (13), the relationship between carbon activity and dewpoint will be determined.

$$\text{Dew point} = \frac{5422.18}{14.7316 - \ln P_{H_2O}} - 273.16 \quad (12)$$



$$\Delta G^0 = -135800 + 143.5 T \quad j$$

$$\Rightarrow \frac{a_c \cdot P_{H_2O}}{P_{H_2} \cdot P_{CO}} = \exp(-17.26 + 16333.895/T) \quad (13)$$

The software developed uses the above-mentioned equations to obtain the required data. In order to confirm the data obtained from the software, a heat treatment furnace (Carbosib202, SIB) was used. The specifications of the furnace and the composition of the methane gas used in the furnace are shown in Tables 1 and 2, respectively.

Table 1. Specifications of the furnace used (Carbosib 202).

Heating power	24 KW
Max Absorption	36.5 A
Max Working Temperature	950 C
Useful Chamber Volume	25 dm <sup>3</sup>

### 3- Results and Discussion

This study aims to conduct the thermodynamic simulation of gaseous reactions using Matlab software in order to easily obtain the carbon weight percent in equilibrium with furnace atmosphere (carbon percent on the part's surface) without performing time consuming calculations.

This is achieved by feeding the relevant parameter inputs such as furnace temperature, furnace pressure, air/fuel ratio, and ambient temperature and humidity into the software developed. The program is capable of generating useful information and applicable curves for furnace conditions once the gas carburizing experimental and environmental variables are supplied. Figure 1 illustrates the main page of the software and Figure 2 provides a schematical view of all the input and output of the software.

Table 2. Composition of the gas used in the furnace.

Methane	Ethane	propane	Iso Butane	n Butane	Iso pentane	n Pentane	n Hexane	Carbon dioxide	H <sub>2</sub> S ppm	Nitrogen
%98.4	%0.66	%0.07	%0.03	%0.03	%0.04	%0.04	%0.12	%0.13	1.7	%0.49



Fig. 1. The main page of the software developed.

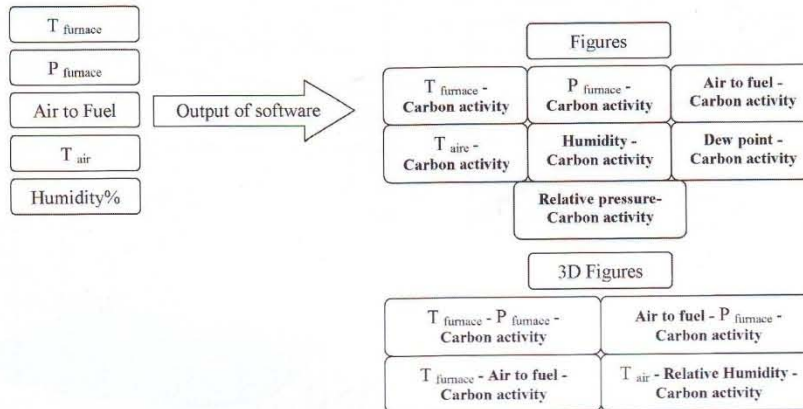


Fig. 2. Schematic view of all the software input and output.

Figure 3 shows the dew point vs. surface carbon percent at 927 °C, 1 atmosphere pressure, and an air-to-fuel ratio of 2.51 to 2.6. As can be seen, the carbon percent increases with decreasing dew point. The data presented here are in good agreement with experimental data published in the literature<sup>1)</sup>.

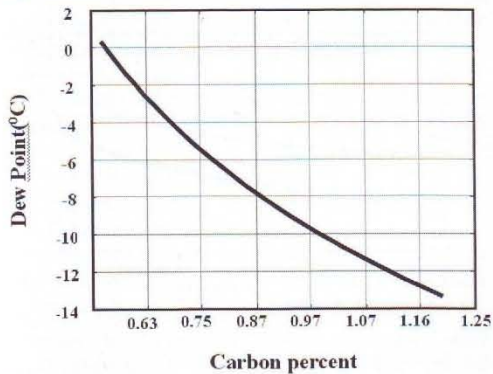


Fig. 3. Dewpoint vs. surface carbon percent at 927 °C, 1 atmosphere, and 2.51- 2.6 air/fuel ratio.

Figure 4 shows surface carbon activity changing with  $P_{CO_2}/P_{CO}$  ratio at 927 °C, 1 atmosphere, and an air-to-fuel ratio of 2.51 to 2.53. As can be seen, surface carbon activity decreases with increasing  $P_{CO_2}/P_{CO}$  ratio due to the progress of Boudouard reaction toward carbon monoxide production. The progress in the opposite direction is explained by the Lechatelier principle, leading to a decrease in the surface carbon content.

Figure 5 shows surface carbon activity changing with air-to-fuel ratio at 927 °C and 1 atmosphere. The amount of methane increases with increasing air-to-fuel ratio according to reaction (1). Consequently, the reaction tends toward the right side according to reaction (2) and the Lechatelier principle which, in turn, results in the reduced amount of  $CO_2$  and increased quantity of  $CO$ , thereby decreasing carbon activity in the Boudouard reaction.

The calculated value of air-to-fuel ratio (using the software developed in this study) and the corresponding experimental value reported in<sup>1)</sup> are 2.508 and 2.5, respectively, which clearly indicate

teh capability of the program in accurately calculating the equilibrium reactions.

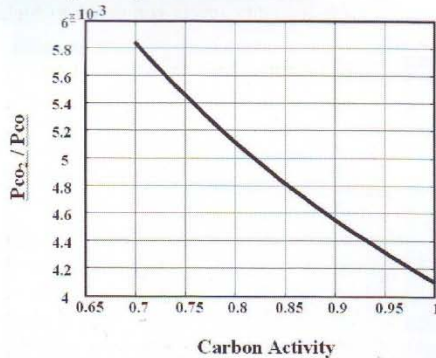


Fig. 4. Surface carbon activity vs.  $P_{CO_2}/P_{CO}$  ratio at 927°C, 1 atmosphere, and 2.51- 2.53 air/fuel ratio.

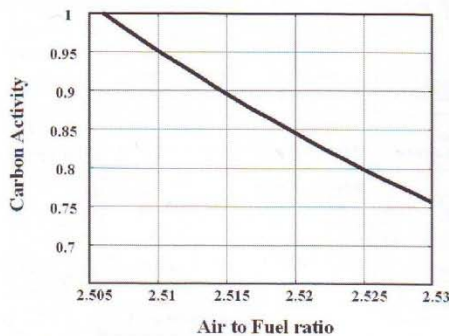


Fig. 5. Surface carbon activity vs. air/fuel ratio at 927 °C and 1 atmosphere.

Figure 6 shows simultaneous changes of carbon activity versus furnace pressure and air-to-fuel ratio at 927 °C. This 3D curve illustrates that at a low air-to-fuel ratio close to 2.5, the change of pressure has a negligible effect on carbon activity (about 0.001), while at higher ratios, changes in furnace pressure alter the furnace potential to a great extent. In fact, one advantage of keeping air-to-fuel ratio at 2.5 in carburizing furnaces is that sudden changes in furnace pressure do not change the furnace potential.

Figure 7 shows simultaneous changes of carbon activity versus furnace temperature and air-to-fuel ratio at a pressure of 1 atmosphere. This 3D curve shows that the furnace potential increases with decreasing temperature. It should also be noted that changing the temperature causes more severe changes in the furnace potential at higher air-to-fuel ratios, while at lower ratios, the changes in temperature have less effects on furnace potential.

Figure 8 shows the changes in dew point with changing air-to-fuel ratio for the experimental results of the gas carburizing furnace at 990 °C, a pressure of 1 atmosphere, an ambient temperature of 24 °C, and a

relative humidity of 65%. The Figure also presents the simulation results by the software for dry air (negligible humidity) and humid air under the same working and environmental conditions. It is observed that a very good agreement exists between the predicted curve for humid air and that obtained from experimental furnace results under the above-mentioned conditions. In all curves, the dew point decreases with decreasing air-to-fuel ratio.

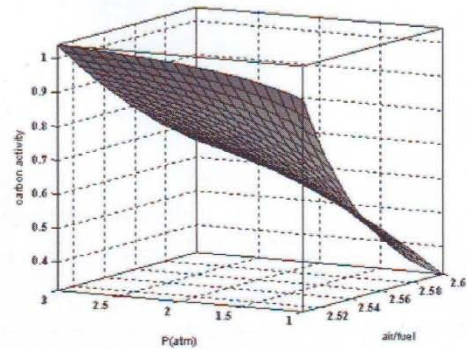


Fig. 6. Simultaneous changes of carbon activity vs. furnace pressure and air/fuel ratio at 927°C.

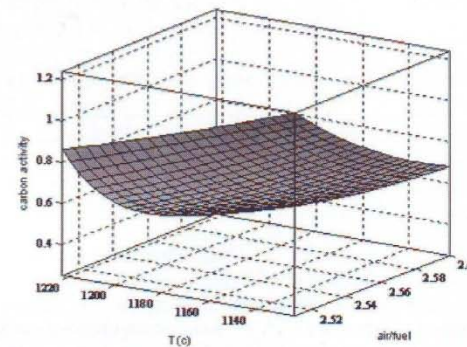


Fig. 7. Simultaneous changes of carbon activity vs. furnace temperature and air/fuel ratio at 1 atmosphere.

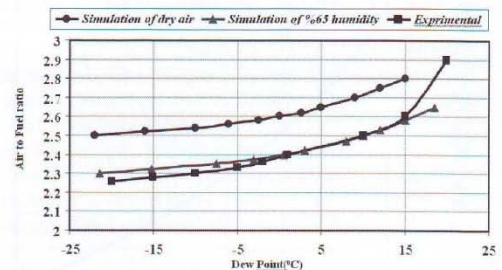


Fig. 8. Variations in dewpoint with changes in air/fuel ratio under experimental and simulated conditions for dry and wet air at 990 °C, 1 atmosphere, and ambient temperature of 24 °C and relative humidity of 65%.

Figure 9 shows the changes in surface carbon percent as a result of changes in air-to-fuel ratio for experimental results obtained from the gas carburizing furnace at 880 °C, 1 atmosphere, an ambient temperature of 21°C, and a relative humidity of 65%. It also shows the simulation results for dry air (negligible humidity) and humid air under the same working and environmental conditions. As can be seen, a very good agreement exists between the predicted curve for humid air and the one obtained from furnace results. In addition, when humid air is compared with dry air under the same conditions, a considerable decrease is observed in the surface carbon percent. The decrease at lower air-to-fuel ratios close to 2.5 is greater than that at higher ratios.

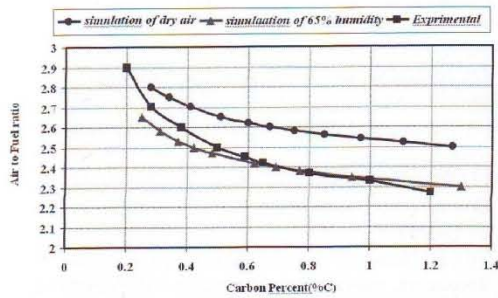


Fig. 9. Variations in carbon percent with changes in air/fuel ratio under experimental and simulated conditions for dry and wet air at 880 °C, 1 atmosphere, ambient temperature of 21 °C, and relative humidity of 65%.

Figure 10 shows the changes of surface carbon activity versus relative humidity of the environment at 1 atmosphere, 927 °C, an air-to-fuel ratio of 2.508, and an ambient temperature of 30 °C. It is observed that carbon activity decreases with increasing humidity, which results in a considerable decrease in gas carburizing efficiency. The reason for this is the increased partial pressure of water as a result of increased humidity ( $P_{H_2O}^*$ ) which causes  $P_{H_2O}$  inside the furnace to increase. According to equilibrium reaction (14), the reaction tends to the right side with an increase in  $P_{H_2O}$  according to the Lechatelier principle resulting in decreased carbon activity.



The following solutions may be recommended to compensate for the severe decrease in carbon activity:

1. Lowering furnace temperature;
2. Increasing furnace pressure; and/or
3. Decreasing air-to-fuel ratio.

Figure 11 shows the simultaneous effect of the ambient relative humidity and temperature on surface carbon activity at 927 °C, an air-to-fuel ratio of 2.51, and a pressure of 1 atmosphere. It is clear that increased humidity results in more severe decreases in carbon activity at ambient temperatures higher than 15 °C compared with lower temperatures (close

to 0 °C). In addition, the effect of ambient temperature on surface carbon activity is less strong at low relative humidity levels compared to higher ones.

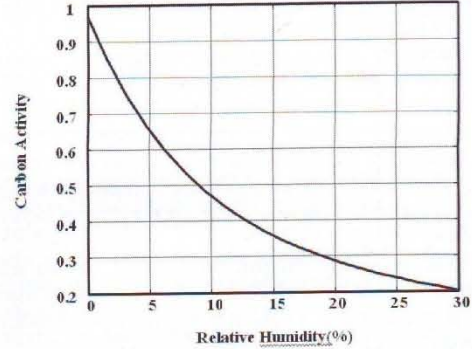


Fig. 10. Surface carbon activity vs. ambient relative humidity at 1 atmosphere, 927 °C, air/fuel ratio of 2.508, and ambient temperature of 30 °C.

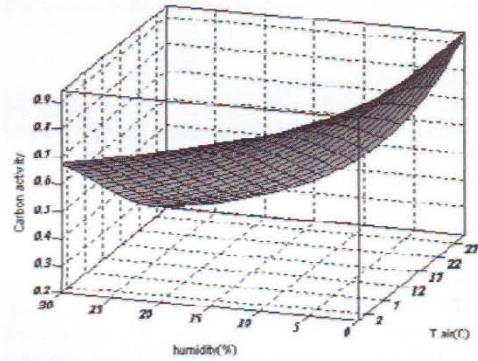


Fig. 11. Effects of simultaneous changes of ambient relative humidity and temperature on surface carbon activity at 927 °C, air/fuel ratio of 2.51, and 1 atmosphere.

The results also indicate that the software developed for this study is capable of rapidly calculating the changes in furnace carbon potential as a result of changes in all the variables affecting gas carburizing.

#### 4- Conclusion

The simulation data generated by the software computations are in good agreement with experimental results of a gas carburizing furnace and the existing theoretical/practical results. Among the significant results obtained from the present study, the following can be highlighted:

- Surface carbon percent of the carburized part increases with decreasing dew point of the furnace gas, air-to-fuel ratio, and carburizing temperature, but with increased pressure inside the carburizing furnace. Moreover, changes in pressure have

negligible effects on carbon activity at air-to-fuel ratios close to 2.5.

- The dewpoint considerably increases in humid air as compared with dry air under identical conditions in which the increase at lower air-to-fuel ratios close to 2.5 is greater than at higher ratios.
- Humidity causes a greater decrease in carbon activity at ambient temperatures higher than 15 °C than at lower temperatures (close to 0 °C).
- Surface carbon percent decreases more considerably in humid air than in dry air under identical conditions in which the decrease at lower air-to-fuel ratios close to 2.5 is greater than at higher ratios.
- The effect of ambient temperature on surface carbon activity is much lower at lower humidity than at higher humidity levels. It is negligible at humidity levels lower than 5%.
- The software developed in this study may be equally used for educational purposes as it can be used effectively and time-efficiently to investigate the effects of different parameters on surface carbon percent without the need to perform time-consuming calculations.

#### 5- Acknowledgments

The authors extend their thanks to the Department of Basic Research, Ministry of Industries & Mines of

Iran for their financial support and to the MST's Industrial Division and its heat treatment section (PGS) for their support in making the gas carburizing furnace available.

#### References

- [1] ASM Metals Handbook, Vol. 4, Heat Treating, (1991).
- [2] David R. Gaskell: Introduction to Thermodynamics of Materials, McGraw-Hill, (1981).
- [3] D.-Y. Ju, C. Liu, T. Inoue, J. Mater. Proc. Tech., 143 (2003), 880.
- [4] B. L. Ferguson, Z. Li, A. M. Freborg, Comp. Mater. Sci., 34 (2005), 274.
- [5] T. Turpin, J. Duley, and M. Gantois, Metall. Mater. Trans. A, 36A (2005), 2751.
- [6] Olga Karabelchtchikova, Richard D. Sisson, J. Phase Equilib. Diff., 27 (2006), 598.
- [7] V. K. Sinha, R. S. Prasad, A. Mandal, and J. Maity, J. Mater. Eng. Performance, 4 (2007), 461.
- [8] H. Jimenez, M. H. Staia, E. S. Puchi, Surf. Coat. Tech., 120-121 (1999), 358.
- [9] F. F. P. de Medeiros, A. G. P. da Silva, C. P. de Souza, U. U. Gomes, Int. J. Refract. Met. H. Mater., 27 (2009), 43.
- [10] R. Nemenyi: Controlled Environments in Heat Treatment, publications of Ferdowsi University of Mashhad, (1377), 81.